**Showcasing research from Professor Lochab's Materials Chemistry Laboratory, Department of Chemistry, School of Natural Sciences, Shiv Nadar University, Uttar Pradesh, India**

Synthesis and thermal behaviour of thiophene-based oxazine-ring substituted benzoxazine monomers & polymers

Owing to their structural design, thiophene-linked 4th generation benzoxazines hold great promise as an emerging class of high performance polybenzoxazine thermosets, as reflected by very high thermal stability and char yield along with minimal mass loss during polymerization.
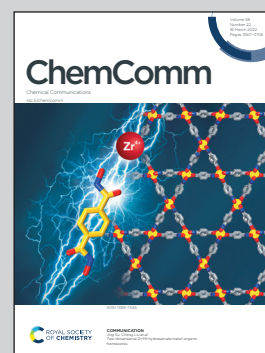
ROYAL SOCIETY
OF **CHEMISTRY**

rsc.li/chemcomm

Synthesis and thermal behaviour of thiophene-based oxazine-ring substituted benzoxazine monomers & polymers†

Sourav Mukherjee [iD] and Bimlesh Lochab [iD] *

The latest fourth-generation oxazine-ring substituted thiophene-based benzoxazine monomers and polymers with variation in the degree of phenyl substitution (with and without) in the oxazine-ring were synthesized and characterized. Thiophene-based di-substituted benzoxazine undergoes ring-opening polymerization at a low temperature with a minimal mass loss during polymerization as supported by molecular geometry-guided intramolecular interactions. This class of monomers provides ample opportunities to design at the molecular level high-performance polybenzoxazines with promising smart applications.

One-pot condensation of phenol and a primary amine with formalin produces 1,3-benzoxazine monomers (BZ), which contain a heterocyclic six-membered oxazine ring with oxygen and nitrogen atoms at the 1- and 3-position. BZ undergoes cationic ring-opening polymerization (ROP) to form polybenzoxazines (PBZs).[1] PBZs offer attractive tuneable properties owing to various advantages *e.g.*, excellent mechanical strength, thermal stability, durability under humid environments, high char yield, long shelf-life, near-zero volumetric expansion or shrinkage, and VOC free (formalin and ammonia) polymerization to suit a variety of applications.[2] The ease of flexible molecular design prompted researchers to develop new scaffolds to affect either the properties and/or ROP temperature. In this regard, several modifications in the monomer structure have been reported, including utilization of a sustainable feedstock.[3] In this direction, furfurylamine has received great attention owing to its biomass origin, polysaccharides, as a congener from the top ten value-added chemicals. The high reactivity offered by furan provides richness in cross-link density in the polymer network.[4] Besides covalent scaffold growth, extensive secondary interactions developed during polymerization lead to rapid development of the mechanical and physical properties[5] of the polymer, such as high glass transition

temperature, hydrophobicity, and thermal stability, which can further be affected by knitting additional heteroatoms (Si, P, N, S, O, *etc.*) in the monomer.

In recent years, efforts to incorporate sulfur into thermosets have gained attention. In this direction, the effect of intermolecular reactions of benzoxazines with thiols and elemental sulfur has been reported.[6] Thiols are known to assist in the ring-opening reaction of benzoxazine, while elemental sulfur acts as the co-monomer to form poly(benzoxazine-*co*-sulfur) copolymers. Poly(benzoxazine-*co*-thiophene) prepared by oxidative copolymerization exhibited conductivity and high thermal stability.[7] Replacement of the oxazine-ring oxygen with the sulfur atom to form polybenzothiazine has also been reported.[8] More recently, disulfide bridges in BZ are introduced for self-healing applications[9] and *in situ* structure modulation of oxazine to thiazine, as a new possible monomer structure.[10] However, covalently-linked sulfur in the BZ scaffold remained elusive.

Furan ring containing PBZs revealed improved thermal performances due to structural interactions. Thiophene can likewise be more participative in polymer network growth due to its high reactivity by virtue of π-excessive heteroaromatics and thus may offer additional reactive sites to influence the properties. This heteroatom substitution hitherto has not been well explored in this domain. Herein, we report the synthesis and characterization of thiophene-based oxazine-ring substituted latest 4th generation benzoxazine monomers. Oxazine-ring substitution at the 2-position (mono-substituted, PH-ta-[2]ph) and 2,4-position (di-substituted, PH-ta-[2,4]ph) with phenyl groups are synthesized and the results are compared with those of the unsubstituted monomer (PH-ta), including polymerization studies.

The synthetic approach for the preparation of monomers with and without oxazine-ring substitution, PH-ta, PH-ta-[2]ph, and PH-ta-[2,4]ph, is shown in Fig. 1. Un- and di-substituted symmetrical benzoxazines, *i.e.*, PH-ta and PH-ta-[2,4]ph, were synthesized using a multicomponent one-pot reaction of phenol (PH) and 2-thiophenemethylamine (ta) with formaldehyde

Materials Chemistry Laboratory, Department of Chemistry, School of Natural Sciences, Shiv Nadar University, Gautam Buddha Nagar, Uttar Pradesh 201314, India. E-mail: bimlesh.lochab@snu.edu.in
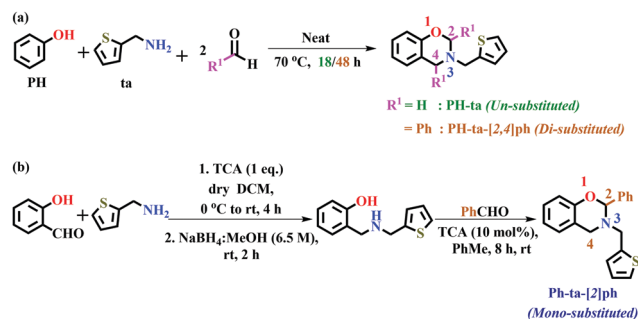
Fig. 1 Synthesis of oxazine ring-substituted thiophene-based benzoxazine monomers.

or benzaldehyde under neat conditions, respectively. While mono-substituted 1,3-benzoxazine, PH-ta-[2]ph was synthesized using a two-step process. Firstly, (thiophenyl)aminophenol was synthesized by reductive amination of salicylaldehyde with "ta" using a trichloroacetic acid (TCA)-mediated condensation reaction followed by treatment with sodium borohydride in methanol. Secondly, condensation of (thiophenyl)aminophenol with benzaldehyde in the presence of catalytic TCA in toluene at room temperature for 8 h furnished the desired mono-substituted benzoxazine. Synthetic protocols are provided in the ESI.†

The structures of the starting material, *viz.*, (thiophenyl)-aminophenol, and benzoxazine monomers, *viz.*, PH-ta, PH-ta-[2,4]ph, and PH-ta-[2]ph, were confirmed using nuclear magnetic resonance (NMR) spectroscopy as shown in Fig. S1–S4 (ESI†). In PH-ta, the characteristic methylene protons were observed as a singlet signal at 4.91 (H_2), 4.03 (H_4), and 4.13 (H_A) ppm due to O–CH_2–N, Ar–CH_2–N, and N–CH_2–Th of the benzoxazine ring and covalently-linked thiophene ring, respectively. The difference between the oxazine-ring proton resonances, $\Delta(\delta_{H2-H4})$, remains unaffected due to the incorporation of the thiophene ring in PH-ta, which lies in the usual range (0.8–0.9 ppm) of typical benzoxazines. However, a relatively significant downfield shift of N–CH_2–Th protons is observed compared to N–CH_2–Fu (3.97 ppm)[4] suggesting a difference in magnetic environment induced by thiophene *vs.* the furan ring. Phenyl substitution at either the 2- or 2,4-position resulted in substantial magnetic inequivalence within the oxazine σ-framework. In PH-ta-[2]ph, the geminal protons in N–CH_2–Ar (H_4, 3.88–3.89 ppm, ^2J = 2 Hz) and N–CH_2–Th (H_A, 3.93–4.04 ppm, ^2J = 28 Hz) appeared as a doublet and doublet of doublets, respectively, due to the induced molecular asymmetry. On the other hand, O–CH(Ph)–N (H_2) is further deshielded due to the anisotropic effect of the phenyl ring at the 2-position and observed as a singlet at 5.97 ppm compared to PH-ta. In PH-ta-[2,4]ph, N–CH(Ph)–Ar (H_4, 5.06 ppm) appeared as a singlet and was significantly deshielded compared to PH-ta-[2]ph. On the contrary, an upfield shift due to dual anisotropy of the two phenyl rings at the 2- and 4-position is noticed in both O–CH(Ph)–N (H_2, 5.79 ppm) and N–CH_2–Th (H_A, 3.68–3.94 ppm, ^2J = 88 Hz). The $\Delta(\delta_{H2-H4})$ ppm in PH-ta-[2]ph increased to 2.08 ppm and decreased to 0.73 ppm

in PH-ta-[2,4]ph, which is close to that observed in PH-ta (0.78 ppm), indicating a pronounced effect of phenyl groups on the electronics of the oxazine ring. The resonance values for carbons C_2, C_4, and C_A in PH-ta, PH-ta-[2]ph, and PH-ta-[2,4]ph are observed at 81.96, 49.54 and 50.59 ppm, 89.86, 47.04 and 48.94 ppm, and 85.14, 60.15 and 45.19 ppm, respectively, reconfirming the successful synthesis of the monomer. NMR studies confirmed that oxazine ring protons are drastically influenced by the presence and number of phenyl substituents as compared to monomers without substitution as indicated by the variation in $\Delta(\delta_{H2-H4})$. This suggests that substituents at the oxazine ring have a strong influence on the electronics at the O–CH(H/Ph)–N reactive centre.

The polymerization reaction of benzoxazine monomers occurs by the heterolytic cleavage at the oxazine ring **O–CH$_2$** or **O–CH(Ph)** bond and hence comprehensive structural elucidation is furthermore required to understand the stereo-electronics of the oxazine ring and its surrounding centres. Therefore, explaining the splitting pattern of **H_A** and **H_2** in PH-ta-[2]ph, and **H_A** in PH-ta-[2,4]ph, and identifying substituted phenyl ring *ortho*-protons (**H_G**) and associated carbons (**C_G**) demand a detailed analysis of 2D NMR [^{1}H–^{1}H COSY (correlation spectroscopy), ^{1}H–^{13}C HMBC (heteronuclear multiple bond correlation) and ^{1}H–^{13}C HSQC (heteronuclear single quantum correlation)] and ^{13}C DEPT (distortionless enhancement by polarization) spectroscopy. ^{1}H–^{1}H COSY 2D NMR of PH-ta-[2,4]ph is displayed in Fig. 2a where the cross-peaks due to methylene protons (**H_A**) and phenyl ring protons (**H_G** and **H_I**) are observed at 3.91 and 3.71, and 7.68 and 7.37 ppm, respectively. This supported the geminal (**H_A**) and vicinal (**H_G** and **H_I**) coupling between the respective protons. Fig. 2b shows the DEPT spectra, where methylene (**C_A**), methine (**C_2** and **C_4**), and quaternary (**C_B**, **C_F**, **C_M**, **C_R**, and **C_S**) carbons are identified using excitation angle 45°, 90° and 135°. The C_2 and C_4 are assigned at 85.04 ppm and 60.02 ppm based on their electronic environment, respectively. The phenyl ring *ortho*-protons (**H_G** and **H_T**)
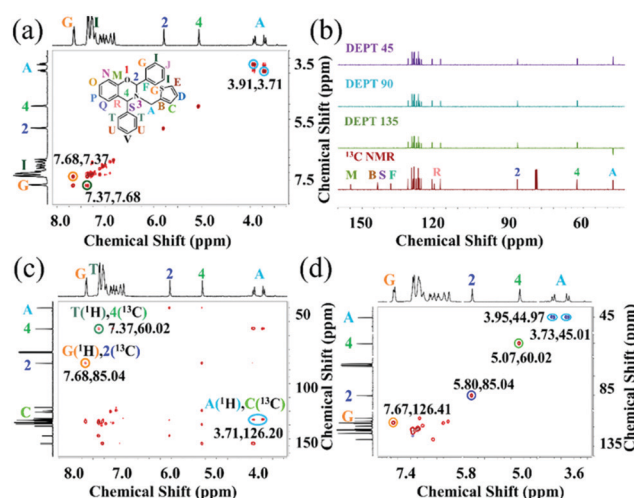

Fig. 2 NMR spectra of PH-ta-[2,4]ph: (a) 2D ^{1}H–^{1}H COSY; (b) stacked ^{13}C and DEPT 45/90/135; (c) 2D ^{1}H–^{13}C HMBC; (d) 2D ^{1}H–^{13}C HSQC.

and H_A were identified using ^{1}H–^{13}C HMBC (Fig. 2c) as cross-peaks noticed from the three-bond coupling between H_G and C_2 (7.68, 85.04 ppm), H_T and C_4 (7.37, 60.02 ppm) and H_A and C_C ($\sim$3.71, 126.20 ppm). ^{1}H–^{13}C HSQC (Fig. 2d) showed one-bond correlation cross-peaks of geminal diastereotopic H_A's with C_A (3.95, 44.97 ppm and 3.73, 45.01 ppm), H_4 with C_4 (5.07, 60.02 ppm), H_2 with C_2 (5.80, 85.04 ppm), and H_G with C_G (7.67, 126.41 ppm). Similarly, the assignment of characteristic protons and carbons for PH-ta and PH-ta-[2]ph (Fig. S1 and S3, ESI†) was achieved by analyzing their 2D-NMR spectra (Fig. S5 and S6, ESI†). Likewise in PH-ta-[2,4]ph, the H_G and C_G resonate at 7.63 and 126.60 ppm, respectively. An unexpectedly high downfield shift of the H_G's in the substituted monomers is suggestive of their spatial interaction with the oxazine ring. The chemical structures of the starting material and monomers are also supported by HRMS analysis (Fig. S7–S10, ESI†). Additionally, Raman spectra were also recorded to further support the formation of monomers (Fig. S11, ESI†).

Only monomer PH-ta-[2,4]ph could be recrystallized (Fig. 3a and Table S1, ESI†), and revealed a short noncovalent distance and bond angle between the plane of the O-atom in the oxazine ring and aromatic ring at the 2-position [O$\cdots$$H_G$–$C_G$ (2-phenyl ring) = 2.428 Å and O$\cdots$H–C = 99.85°]. Natural Bond Orbital (NBO) analysis of PH-ta-[2,4]ph using theoretical calculations at the B3LYP/6-31(d,p)[11] level of theory revealed the existence of weak intramolecular non-covalent interactions between the nO (oxazine ring) → σ* (phenyl C–H_G), as depicted in Fig. 3b with second-order perturbation energy, $E^{(2)}$, equal to 0.62 kcal mol^{-1}.[12] Likewise, intramolecular 5-membered H-bonding interactions influence the rate or temperature of polymerization.[13] This nonbonding orbital interaction may account for the diminished bond strength of the C–H_G in the phenyl ring (compared to other protons in the Ph-ring) validating the observed downfield chemical shift in NMR. Additionally, the presence of inter-molecular CH-π (Fig. S12, ESI†) interactions is also observed.

To determine the effect of phenyl-substituents on ROP temperature, differential scanning calorimetry (DSC) analysis was performed (Fig. 4a). DSC thermograms revealed a sharp melting (melting temperature, T_m) endothermic transition at 67 °C (PH-ta), 106 °C (PH-ta-[2]ph), and 118 °C (PH-ta-[2,4]ph) confirming the high purity of the monomers. Exothermic transition due to oxazine-ring opening polymerization (peak temperature of polymerization, T_p) followed the order PH-ta-[2,4]ph (211 °C) < PH-ta-[2]ph (224 °C) < PH-ta (242 °C). It is
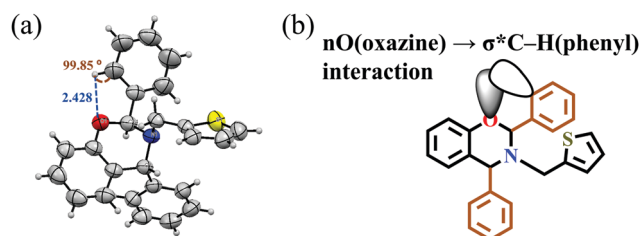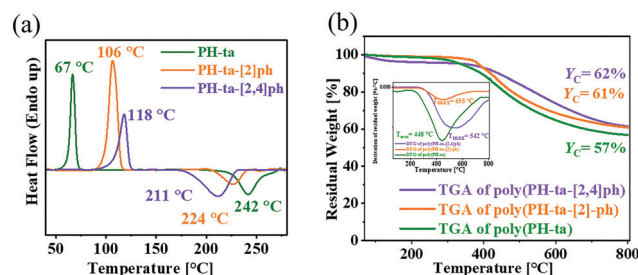

Fig. 4 (a) DSC of the monomers and (b) TGA and DTG (inset) thermograms of the polymers.

evident from the shift in the baseline of the polymerization exotherm (initiation temperature, T_i), that the O–CH(Ph)–N bond cleavage in the oxazine ring to form an iminium ion intermediate was initiated at a further low temperature. The T_i values were determined as 176 °C, 204 °C and 219 °C for PH-ta-[2,4]ph, PH-ta-[2]ph, and PH-ta, confirming the significant role of phenyl in abetting the lowering of the ROP temperature. A slight broad endotherm and exothermic transition in PH-ta-[2,4]ph is attributed to the fast ring-opening reaction and the so formed phenolic hydroxyl group autocatalyzes the ring-opening reaction of the benzoxazine monomer.

The processing window of all the monomers, where the monomers melt and reach a stage where they can be easily moulded, is sufficiently wide, which is beneficial for the preparation of composites (Table S2, ESI†). The heat of polymerization (ΔH, kJ mol^{-1}) for the monomers is also found to be affected by phenyl ring substitution, and the value obtained is the highest in PH-ta-[2,4]ph, suggesting the participation of the phenyl and thiophene rings in the cross-linking reactions. Intriguingly, the presence of a flexible methylene linker, between the N in the oxazine and thiophene ring in the monomer, maximizes conformational freedom for the enhanced participation of thiophene in electrophilic aromatic cross-linking reactions. Surprisingly, the ΔH value obtained is slightly lower for PH-ta-[2]ph than PH-ta implying that the stability and steric hindrance of the ring-opened iminium ion intermediate governs the ring-opening and polymerization process. The activation energy (E_a) values for the observed polymerization exotherm, the DSC kinetic study, were determined using Kissinger and Ozawa plots (Fig. S13 a–f, ESI†), and the values obtained are in good agreement. The E_a value follows the order PH-ta (79 kJ mol^{-1}) < PH-ta-[2]ph (92 kJ mol^{-1}) < PH-ta-[2,4]ph (112 kJ mol^{-1}). Qualitative analysis of FTIR of the monomers when heated at variable temperatures (Fig. S14, ESI†) also supported a fast ring-opening reaction (above 170 °C) as implied by the significant broadening and vanishing of characteristic oxazine related [O–CH(H/Ph)–N] vibrational bands correlating with the structural dependence on the monomers.

During polymerization, mass losses are often observed, which is one of the pressing issues. To probe whether with the incorporation and increase in the number of phenyl ring(s), from PH-ta to PH-ta-[2]ph and further to PH-ta-[2,4]ph,

Fig. 3 (a) ORTEP diagram of the crystal structure of PH-ta-[2,4]ph. Interactions: (b) intramolecular nO → σ* C–H_G interaction.

imparted thermal stability to the monomers, thermogravimetric analysis (TGA) of the monomers was performed. As it can be seen in the thermogravimetry/differential thermogravimetry (DTG) thermograms (Fig. S15, ESI†), the T_{max} (temperature of maximum mass loss) value increased with the increase in phenyl substitution in the monomer. This may be attributed to the increase in (i) molecular mass of the monomer and (ii) extensive through space nuclear Overhauser effect (NOE) interactions as supported from ^1H–^1H NOESY spectra (Fig. S16–S18, ESI†).[14] In the case of PH-ta-[2,4]ph, such intramolecular cross-interactions were intensified among the aromatic protons ($H_{G/I/J}$ and H_T) of both the phenyl rings at the 2- and 4-position noticed to further interact with other characteristic oxazine-ring protons of aliphatic centres ($H_{2/4/A}$) as well as the thiophenyl ring ($H_{C/D}$). Additionally, extensive CH-π intermolecular interactions in PH-ta-[2,4]ph, provided extra thermal stability in comparison to the other structures. Combined analysis of T_{max}, T_p, ΔH, and E_a values inferred that among all the monomers, PH-ta-[2,4]ph undergoes a fast ring-opening reaction due to the stabilization of the iminium ion intermediate (extended to benzylic carbocation) accounting for the lowest T_p but may suffer from steric retardation in the polymer propagation reactions owing to the initial extensive involvement of aromatic rings in the cross-linking reaction as indicated from the highest E_a value. However, the highest ΔH indicates that the so-formed 3D polymer network of poly(PH-ta-[2,4]ph) is probably highly cross-linked and thermodynamically stable.

The conversion of monomer to polymer was achieved by thermal treatment of the monomers (when cured at their T_p) in an air oven. After confirmation of complete polymerization of the monomers, as noticed from no solubility of the cured polymer in chloroform and dimethyl sulfoxide, the samples were subjected to TGA to examine the thermal stability of the polymers. The TGA/DTG curves (Fig. 4b) of the polybenzoxazines displayed an initial thermal stability (5% and 10% mass decomposition temperatures i.e., $T_{d5\%}$ = 334–384 °C and $T_{d10\%}$ = 393–439 °C), maximum mass loss temperature (T_{max} = 448–542 °C) and char yield at 800 °C (57–62%) which is significantly higher than furan based monomers[15] (Table S3, ESI†). This indicates the possible extensive participation of the thiophenyl ring in polymerization leading to a highly thermally stable thermoset (Fig. S19, ESI†). The limiting oxygen index (LOI) values, one of the criteria for flame resistance, were calculated using the Van Krevelan and Hofytzer equation. The calculated LOI value of the thiophene-based polymers falls in the range of 40.3–42.3 (LOI $\leq$ 28 is considered flammable). A very high LOI, char yield, and initial thermal stability make this class of thiophene-based polymers stand out with inherent self-extinguishable nature owing to the presence of nitrogen and sulfur atoms in the monomer. Additionally, such polymer characteristics are obtained from simple facilely synthesized halogen-free monomers classifying them as environmentally safe intrinsic flame-retardant polymers.

To conclude, catalyst-free, neat, and scalable multicomponent reactions using commercially available reactants were employed to construct un-/di-substituted benzoxazines. The properties of the oxazine-ring substituted benzoxazines can be modulated by regulating the nonbonding orbital and NOE interactions. NMR interpretations may be a guiding principle in understanding stereo-electronics, which may pave the way towards structural engineering in this newly emerging class of monomers. It is interesting to note that despite containing only a simple mono-oxazine moiety, the substituted polybenzoxazines still registered exceptionally high thermal performance, which makes such scaffolds worth exploring. A direction may be obtained from the current work towards the investigation of substituted benzoxazines and their composites to gratify a new horizon of high-end applications.

Conflicts of interest

There are no conflicts to declare.

References

1 J. Dunkers and H. Ishida, *J. Polym. Sci., Part A: Polym. Chem.*, 1999, **37**, 1913–1921.
2 (*a*) M. G. Mohamed and S.-W. Kuo, *Macromolecules*, 2020, **53**, 2420–2429; (*b*) B. Lochab, M. Monisha, N. Amarnath, P. Sharma, S. Mukherjee and H. Ishida, *Polymers*, 2021, **13**, 1260; (*c*) Y. Lu, K. W. J. Ng, H. Chen, X. Chen, S. K. J. Lim, W. Yan and X. Hu, *Chem. Commun.*, 2021, **57**, 3375–3378.
3 (*a*) E. Calò, A. Maffezzoli, G. Mele, F. Martina, S. E. Mazzetto, A. Tarzia and C. Stifani, *Green Chem.*, 2007, **9**, 754–759; (*b*) L. Dumas, L. Bonnaud, M. Olivier, M. Poorteman and P. Dubois, *J. Mater. Chem. A*, 2015, **3**, 6012–6018; (*c*) L. Dumas, L. Bonnaud, M. Olivier, M. Poorteman and P. Dubois, *Eur. Polym. J.*, 2016, **75**, 486–494.
4 Y. L. Liu and C. I. Chou, *J. Polym. Sci., Part A: Polym. Chem.*, 2005, **43**, 5267–5282.
5 G. R. Goward, D. Sebastiani, I. Schnell, H. W. Spiess, H.-D. Kim and H. Ishida, *J. Am. Chem. Soc.*, 2003, **125**, 5792–5800.
6 (*a*) I. Gorodisher, R. J. DeVoe and R. J. Webb, in *Handbook of Benzoxazine Resins*, ed. H. Ishida and T. Agag, Elsevier, Amsterdam, 2011, pp. 211–234; (*b*) A. W. Kawaguchi, A. Sudo and T. Endo, *J. Polym. Sci., Part A: Polym. Chem.*, 2014, **52**, 1448–1457; (*c*) S. Shukla, A. Ghosh, P. K. Roy, S. Mitra and B. Lochab, *Polymer*, 2016, **99**, 349–357; (*d*) M. Arslan, B. Kiskan and Y. Yagci, *Macromolecules*, 2016, **49**, 767–773.
7 B. Kiskan, Y. Yagci, E. Sahmetlioglu and L. Toppare, *J. Polym. Sci., Part A: Polym. Chem.*, 2007, **45**, 999–1006.
8 S. Ohashi, E. Rachita, S. Baxley, J. Zhou, A. Erlichman and H. Ishida, *Polym. Chem.*, 2021, **12**, 379–388.
9 A. Trejo-Machin, L. Puchot and P. Verge, *Polym. Chem.*, 2020, **11**, 7026–7034.
10 M. Monisha, S. Sahu and B. Lochab, *Biomacromolecules*, 2021, **22**, 4408–4421.
11 I. Machado, I. Hsieh, E. Rachita, M. L. Salum, D. Iguchi, N. Pogharian, A. Pellot, P. Froimowicz, V. Calado and H. Ishida, *Green Chem.*, 2021, **23**, 4051–4064.
12 R. S. Rowland and R. Taylor, *J. Phys. Chem.*, 1996, **100**, 7384–7391.
13 P. Froimowicz, K. Zhang and H. Ishida, *Chem. – Eur. J.*, 2016, **22**, 2691–2707.
14 N. Sini and T. Endo, *Macromolecules*, 2016, **49**, 8466–8478.
15 S. Mukherjee, N. Amarnath and B. Lochab, *Macromolecules*, 2021, **54**, 10001–10016.